Design of S-shaped diffusers in incompressible flow

J. L. Sproston*

The hodograph method, in conjunction with a numerical form of the Schwarz–Christoffel transformation, is applied to the determination of the shape of an S-shaped diffuser subject to certain prescribed characteristics in incompressible flow. It is shown how the resulting diffuser of infinite length can be modified to one of finite length by limiting the upstream and downstream velocities to within a small percentage of their normal asymptotic values

Key words: *air intakes, incompressible flow, hodograph methods*

The hodograph method of solving problems of two-dimensional, irrotational flows was first used as long ago as 1868 when Helmholtz[1] investigated aerofoil flows with cavitation. A more recent successful application of the method by Cheers[2] has been to the design of contractions for wind tunnels where the control of velocity gradients, adverse to the development of the boundary layer, was of prime concern. Until very recently, solutions that have been obtained by the hodograph method have been limited to situations where the flow in the hodograph plane could easily be transformed back to the physical plane, a process necessary to establish the (1–1) correspondence. For example, there have been numerous solutions to problems in which the resulting flows in the logarithmic hodograph plane were confined to polygons of 3 or 4 sides. In these cases, analytical solutions, often using the Schwarz–Christoffel transformation, could be generated in terms of either elementary functions or, at worst, in terms of elliptic functions. Of particular interest here is an investigation by Goldstein[3] who indicated how certain types of profile for contracting ducts could result in infinite velocity gradients. Later, Gibbings and Dixon[4] showed that the contraction profile could also possess points of infinite curvature.

The hodograph method has been applied successfully by Gibbings and Sproston[5] and Sproston[6] to the design of aerofoil profiles in which pre-specification of desirable characteristics such as velocity distributions, pressure gradients, radii of curvature have been effected. The present application has been stimulated by the apparent lack of research into the design of more complicated duct shapes, and by the development[7] of a generalized numerical form of the Schwarz–Christoffel transformation.

The S-shaped diffuser became of interest mainly because of its use in aircraft air intakes. The incorporation of bypass cavities into the outer wall of the diffuser was considered by Gerhold[8] as a possible way of reducing or eliminating the risk of damage by ingestion of foreign objects. Because of its higher inertia, incoming debris would usually impinge on the outer wall of the diffuser and a suitably placed cavity could act as a collector. It appeared initially, therefore, that the diffuser shape, without the cavity, should be shown to be derivable from a specification of characteristics which would be of particular significance to the later ingestion problem.

The present analysis is restricted to irrotational, incompressible flow in two-dimensions, but it is important to appreciate that an extension to compressible flow would be facilitated by the linearity of the resulting equations in the hodograph plane.

Analysis

For two-dimensional, incompressible irrotational flow, it is well known that the complex potential is given by $W = \phi + i\psi$. Differentiation with respect to the physical (or diffuser) plane co-ordinate, z, gives:

$$\frac{\mathrm{d}W}{\mathrm{d}z} = qe^{-i\theta} \tag{1}$$

and hence the logarithmic hodograph plane variable:

$$\Omega = \ln(\mathrm{d}W/\mathrm{d}z) = \ln q - i\theta \tag{2}$$

Thus, the diffuser profile in the z-plane (along which $\mathrm{d}\psi = 0$) will have co-ordinates which satisfy the equations:

$$\int \mathrm{d}x = \int \frac{\cos\theta}{q}\,\mathrm{d}\phi \quad \text{and} \quad \int \mathrm{d}y = \int \frac{\sin\theta}{q}\,\mathrm{d}\phi \tag{3}$$

Effectively, therefore, the problem has been reduced to the determination of the velocity potential distribution in the Ω-plane, together with the point-to-point correspondence between the z- and Ω-planes.

As a particular example, it was decided to determine the S-shaped diffuser profile (Fig 1(a))

* Department of Mechanical Engineering, The University of Liverpool, Liverpool, UK, L69 3BX
Received 15 March 1982 and accepted for publication on 4 June 1982

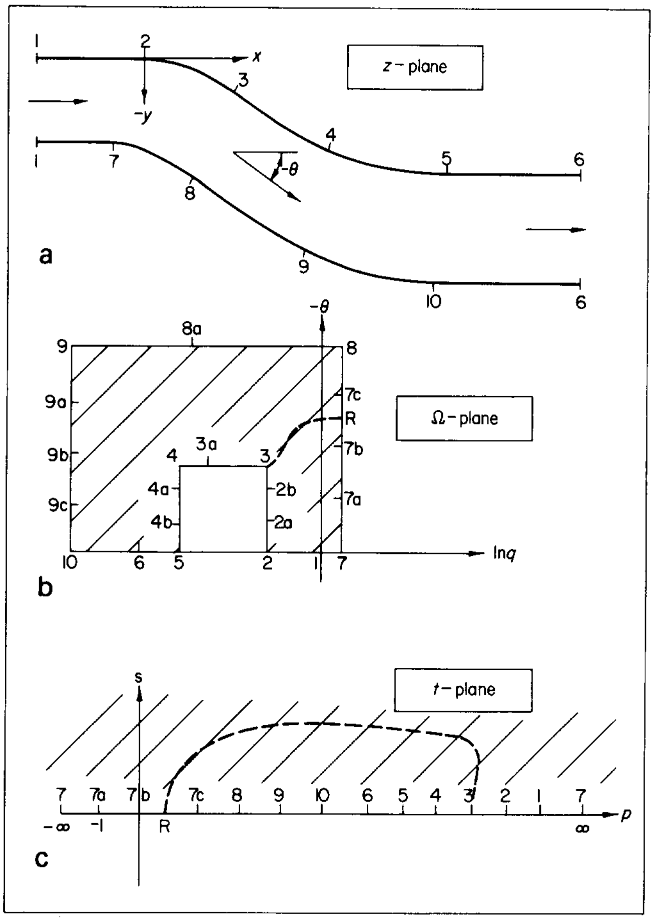

Fig 1 (a) The diffuser plane (b) The logarithmic hodograph plane (c) The auxiliary half-plane

which would correspond with the following prescribed characteristics:

(i) $q_1 = 1$ (ii) $q_2 = q_3 = 0.81$
(iii) $q_4 = q_5 = 0.66$ (iv) $q_6 = 0.635$
(v) $\theta_{3,4} = -13.75°$ (vi) $\theta_{8,9} = -34°$
(vii) $q_7 = q_8 = 1.03$ (viii) $q_9 = q_{10} = 0.486$

where the subscripts refer to numbered points.

In addition, the diffuser boundary is to be designed to consist of straight portions along (1–2), (3–4), (5–6), (1–7), (8–9) and (10–6) and the portions (2–3), (4–5), (7–8) and (9–10) are to be of constant velocity magnitude.

The corresponding Ω-plane of Fig 1(b) consists of a 10-sided polygon whose sides are parallel to one or the other of the co-ordinate axes. (The points marked a, b etc. are for future reference.)

The determination of ϕ as a function of Ω is effected by transforming the interior of the Ω-plane of Fig 1(b) onto the upper half of an auxiliary t-plane of Fig 1(c) so that the boundary of the Ω-plane maps onto the real axis in the t-plane. The transformation is carried out by using a numerical form of the Schwarz–Christoffel Eq (7) developed so that polygons of many sides can be rapidly accommodated.

For convenience the sides of the polygon in the Ω-plane as seen in Fig. 1(b) are sub-divided into shorter sides to produce a 22-sided polygon; thus, when the transformation is established the point-to-point correspondence is found automatically for 22 points.

Considering the flow in the t-plane, it can be seen that it is due to a source at point 1 and a sink at point 6. Hence, taking unit strengths, the complex potential can be written as:

$$W = \ln(t - t_1) - \ln(t - t_6) \tag{4}$$

and the velocity potential as:

$$\phi = \ln\left|\frac{t - t_1}{t - t_6}\right| \tag{5}$$

where t_1 and t_6 are real.

Effectively, therefore, as ϕ is now known as a function of t, and t is known (via the Schwarz–Christoffel transformation) as a function of Ω, it follows from Eq (3) that the x, y-co-ordinates can be determined. However, although the shapes of the upper and lower boundaries can be separately determined, further analysis is required for the determination of their respective positions. This is achieved by determining the z-co-ordinates of two points, one on the upper surface and one on the lower surface, and which are on the same equi-potential line (i.e. a ϕ-line). Along such a ϕ-line it can be seen from Eq (1) that it is possible to express the x- and y-co-ordinates, respectively, as:

$$dx = -\frac{\sin\theta}{q}\,d\psi \quad \text{and} \quad dy = \frac{\cos\theta}{q}\,d\psi \tag{6}$$

If the ϕ-line which passes through point 3 in the Ω-plane (and hence on the upper surface of the diffuser) meets the boundary corresponding to the lower surface at point R in the Ω-plane, then integration of Eq (6) will yield $(x_3 - x_R)$ and $(y_3 - y_R)$. This

Notation

b	Polar angle in t-plane
e	Length of diffuser between points H and 2 (Fig 2)
G	Constant used in Eq (9)
K	Complex scaling constant
L	Overall length of (finite) diffuser
p	Real part of function t
q	Velocity magnitude
r	Polar distance in t-plane
s	Imaginary part of function t
t	Complex variable in half plane
W	Complex potential ($W = \phi + i\psi$)
z	($= x + iy$) Diffuser plane variable
$\bar{x}, \bar{y}$	Dimensionless co-ordinates of diffuser ($\bar{x} = (x + e)/L$, $\bar{y} = y/L$)
Greek characters	
θ	Local flow direction (Fig 1(a))
Ω	($= \ln q - i\theta$) Logarithmic hodograph plane variable
ϕ	Velocity potential
ψ	Stream function

integration can be executed when the position of point R is known in the t-plane and when the right-hand sides of Eq (6) can be expressed as functions of t.

Denoting the value of ϕ at point 3 as ϕ_3, then it follows from Eq (5) that $e^{\phi_3} = |(t-t_1)/(t-t_6)|$. Hence, the locus of $\phi = \phi_3$ in the t-plane is given by $e^{\phi_3} = |[(p-t_1)^2+s^2]/[(p-t_6)^2+s^2]|^{1/2}$ where $t = p+is$. After a little algebraic manipulation this becomes:

$$s^2(1-e^{2\phi_3}) = 2p(t_1 - e^{2\phi_3}t_6) + e^{2\phi_3}t_6^2 - t_1^2 - p^2(1-e^{2\phi_3}) \tag{7}$$

Thus, the s-value can be determined for a given p-value along $\phi = \phi_3$ and in particular the p-value of point R is found by putting $s = 0$ and solving the resulting quadratic equation.

To express the right-hand sides of Eq (6) as functions of t along $\phi = \phi_3$, it is convenient to apply the Schwarz–Christoffel transformation to the polygon in the Ω-plane of Fig 1(b) without the intermediate alpha numeric vertices. When the t-value of point 7 (t_7) is taken conveniently as $-\infty$, the transformation between the Ω- and t-planes can be expressed by:

$$\frac{d\Omega}{dt} = K\left(\frac{(t-t_3)(t-t_4)}{(t-t_2)(t-t_5)(t-t_8)(t-t_9)(t-t_{10})}\right)^{1/2} \tag{8}$$

where K is a scaling constant.

Expressing each of the bracketed terms in the polar form $(t-t_x) = r_x e^{ib_x}$, where $r_x^2 = s^2 + (p-p_x)^2$ and $b_x = \arctan(s/(p-p_x))$, it follows that:

$$\int d\Omega = K\int Q^{1/2}e^{iG}\,dt$$

where

$$Q = r_3 r_4 / r_2 r_5 r_8 r_9 r_{10}$$

and

$$G = (b_3 + b_4 - b_2 - b_5 - b_8 - b_9 - b_{10})/2.$$

Also, as $d\Omega = dq/q - i\,d\theta$, therefore:

$$\int \frac{dq}{q} = K\int Q^{1/2}(\cos G\,dp - \sin G\,ds) \tag{9}$$

and

$$-\int d\theta = K\int Q^{1/2}(\cos G\,ds + \sin G\,dp)$$

Application of the numerical algorithm[7] produces the t-values in Eq (8) and, hence, for a given point along $\phi = \phi_3$ in the t-plane, Eq (9) will give the corresponding values of q and θ. This information, together with the ψ-distribution (along $\phi = \phi_3$) given from Eq (4) in the form $\psi = \arg(t-t_1) - \arg(t-t_6)$, creates the necessary t-functions for the right-hand sides of Eq (6).

Results

After application of the Schwarz–Christoffel transformation to the Ω-plane of Fig 1, the results shown in Table 1 were obtained. It is noteworthy that, in using this transformation, there is a free choice of t-values corresponding to three vertices in the polygon plane and in this case the t-values were chosen for points 7, 7a and 7b.

The p-values for points R and 3 were found to be 0.085 and 0.2975, respectively (which incidentally means that point R lies between points 7b and 7c in the Ω-plane of Fig 1). Together with other arbitrary points in between R and 3 (B, C etc.) whose co-ordinates (p, s) had been computed from Eq (7), Eq (9) was integrated numerically and the (q, θ) values along the curve joining points 3 and R, together with the corresponding values of ψ, are given in Table 2. Also, numerical integration of Eq (6) gave the spacings $(x_3 - x_R)$ and $(y_3 - y_R)$ as -0.993 and 3.374, respectively. Finally, numerical integration of Eq (3) between points 7b and R gives $(x_R - x_{7b})$ and $(y_R - y_{7b})$ as 0.535 and -0.186, respectively. Sufficient information is now available not only to determine the shapes of the upper and lower boundaries of the diffuser, but also their respective positions.

As the resulting profile is of infinite length and the upstream and downstream velocities are asymptotically approached, it is clearly desirable to investigate the case in which a finite length can be attained. Referring to Fig 1, numerical integration of Eq (8) is carried out along the straight portions (1, 2), (1, 7), (5, 6) and (10, 6) to find the t-values of points at which the velocities q (given by e^{Ω} from Eq (2) with $\theta = 0$) are within 0.5% of their respective asymptotic values. Subsequent integration of Eq (3), using Eq (5) for ϕ, gives the corresponding x-co-

Table 1

Point	$\cos\theta/q$	$-\sin\theta/q$	t	ϕ
Upper surface ($\psi = \pi$)				
1	1	0	40.9535	$-\infty$
2	1.2345	0	1.5746	3.3489
2a	1.2295	0.1110	1.1619	3.7137
2b	1.9946	0.2210	0.5633	4.6881
3	1.1991	0.2934	0.2975	5.9499
3a	1.3121	0.3211	0.2111	7.6420
4	1.4784	0.3618	0.1939	9.7610
4a	1.4974	0.2725	0.1921	11.2133
4b	1.5159	0.1368	0.1916	13.6111
5	1.5220	0	0.19156	15.2204
6	1.5968	0	0.19155	∞
Lower surface ($\psi = 0$)				
1	1	0	40.9535	$-\infty$
7	0.9704	0	$-\infty$	0
7a	0.9595	0.1450	-1	3.5613
7b	0.9271	0.2867	0	5.3650
7c	0.8738	0.4221	0.1185	6.3261
8	0.8010	0.5480	0.1370	6.6177
8a	1.1480	0.7850	0.1773	7.9591
9	1.6982	1.1618	0.1879	9.3208
9a	1.8527	0.8960	0.1886	9.5337
9b	1.9657	0.6080	0.1901	10.2439
9c	2.0345	0.3075	0.1909	11.0463
10	2.0570	0	0.1912	11.6653
6	1.5698	0	0.19155	∞

Table 2

Point	ln q	q	θ^0	$\cos\theta/q$	$\sin\theta/q$	ψ
R	0.280	1.0284	−21.2682	0.9061	−0.3527	0
B	−0.0139	0.9862	−20.9186	0.9471	−0.3620	0.3045
C	−0.0310	0.9689	−20.6494	0.9658	−0.3639	0.4426
D	−0.0650	0.9370	−19.2227	1.0077	−0.3513	0.6962
E	−0.1109	0.8950	−17.7502	1.0641	−0.3406	1.1666
F	−0.1456	0.8645	−16.1688	1.1109	−0.3221	1.6544
G	−0.1727	0.8419	−14.6448	1.1492	−0.3003	2.1523
3	−0.2100	0.8106	−13.7510	1.1983	−0.2932	3.14149

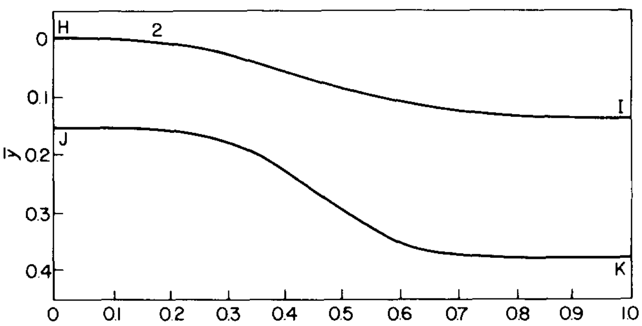

Fig 2 Dimensionless plot of the finite length diffuser

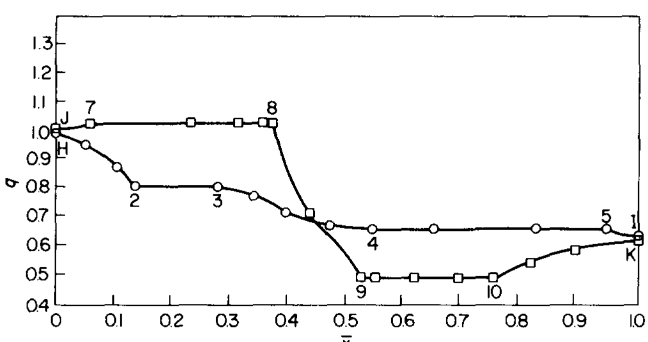

Fig 3 The velocity distribution on the upper and lower boundaries of the diffuser. ○, refers to the upper surface; □, refers to the lower surface

ordinates of these points (H, I, J, K in Fig 2). Numerical values of the (x, y) co-ordinates of the diffuser boundaries (with the origin for both taken at point 2) together with the dimensionless co-ordinates $(\bar{x}, \bar{y})$ are shown in Table 3. Here, $\bar{x}$ and $\bar{y}$ are defined as $\bar{x} = (x + e)/L$ and $\bar{y} = y/L$ where e is the distance between points H and 2, and L is the axial distance between points H and I. The dimensionless plot of the finite diffuser is shown in Fig 2 and the corresponding velocity distribution in Fig 3.

The velocity distribution illustrates some interesting features, first described by Gibbings and Dixon[4], at points on the diffuser walls corresponding to stagnation points in the flow in the Ω-plane. At these points, the velocity gradients are infinite in value, and at the points 2,5 on the upper surface and points 8,9 on the lower surface, the gradients are adverse. In the real flow situation, of course, these gradients could cause boundary layer separation, and would represent, therefore, an undesirable feature of this particular example.

Table 3

Point	x-co-ord	$(-y)$-co-ord	$\bar{x}$	$-\bar{y}$	q
Upper surface					
H	−2.60	0	0	0	0.996
2	0	0	0.129	0	0.81
2a	0.449	0.020	0.152	0.001	0.81
2b	1.640	0.182	0.211	0.009	0.81
3	3.163	0.506	0.287	0.025	0.81
3a	5.287	1.026	0.392	0.051	0.72
4	8.244	1.750	0.539	0.087	0.66
4a	10.405	2.210	0.647	0.110	0.66
4b	14.017	2.701	0.827	0.134	0.66
5	16.442	2.811	0.947	0.140	0.66
I	17.502	2.811	1.000	0.140	0.64
Lower surface					
J	−2.60	3.047	0	0.151	1.004
7	−1.517	3.047	0.054	0.151	1.03
7a	1.919	3.305	0.225	0.164	1.03
7b	3.621	3.694	0.309	0.184	1.03
7c	4.486	4.035	0.352	0.201	1.03
8	4.731	4.176	0.365	0.208	1.03
8a	6.038	5.071	0.430	0.252	0.72
9	7.975	6.396	0.526	0.318	0.486
9a	8.353	6.615	0.545	0.329	0.486
9b	9.709	7.148	0.612	0.356	0.486
9c	11.314	7.516	0.692	0.374	0.486
10	12.581	7.611	0.755	0.379	0.486
K	17.502	7.611	1.000	0.379	0.631

Conclusions

It has been shown, using a numerical form of the Schwarz–Christoffel transformation, how the design of an S-shaped diffuser can be effected. The relatively simple rectilinear shape in the logarithmic hodograph plane facilitated pre-specification of constant velocity and constant angled portions for the diffuser. The very nature of the numerical form of the transformation equally allows virtually any other shape in the Ω-plane to be handled, because the program run-time on a CDC 7600 for the present case was <3 s. Curved boundaries in the Ω-plane present no problem because they are simply represented by a succession of small rectilinear segments. In this respect, the desirable 'rounding-off' of these points in the Ω-plane which gave rise to infinite adverse velocity gradients could be accommodated.

Because of the singularity representation in the Ω-plane of the upstream and downstream conditions in the z-plane, the diffuser, consequently, will be of (doubly) infinite length. The necessary shortening has been shown to be easily accomplished in a way in which the upstream and downstream velocities are specified to be within a small percentage of their asymptotic values.

Although the present analysis is limited to incompressible flows, it is envisaged that a later investigation will extend the method to compressible flows, made possible by the linearity of the flow equations in the Ω-plane. The subsequent conformal transformation will, of course, change the form of the equation, but that might be more than compensated for in easy specification of boundary conditions in the t-plane.

References

1. **Helmholtz H. V.** On discontinuous movements of fluids. *Phil. Mag. Ser. 4, 1868,* **36,** *337*
2. **Cheers F.** Note on wind tunnel contractions. *Aero. Res. Council, Rep. and Mem., 1945, 2137*
3. **Goldstein S.** Notes on the design of converging channels. *Aero. Res. Council, Rep. and Mem., 1945, 2643*
4. **Gibbings J. C. and Dixon J. R.** Two-dimensional contracting duct flow. *Quart. J. Mech. and Appl. Maths., 1957,* **10,** *24*
5. **Gibbings J. C. and Sproston J. L.** The symmetrical aerofoil at zero incidence. *Aero. Res. Council, 1973, 34479*
6. **Sproston J. L.** Double-wedge aerofoils at zero incidence. *Aero Res. Council, 1973, 34480*
7. **Sproston J. L.** A numerical form of the Schwarz–Christoffel transformation. *University of Liverpool, Fluid Mech. Int. Rep. FM/39/77, 1977*
8. **Gerhold M. N.** Aerodynamic performance tests of S-curved diffusers incorporating bypass cavities. *Hawker Siddeley Aviation Int. Rep., 1977, HSA-KGT-R-GEN-00655*

BOOK REVIEWS

Two-phase Flow Dynamics

Edited by A. E. Bergles and S. Ishigai

This book contains twenty-six papers presented at a Japanese–US Seminar on two-phase dynamics held in Kobe, Japan on 31 July–3 August 1979. The papers can be categorised into: surveys, flow regimes, transient analysis, pressure wave propagation, flow instability, choking flow, and loss-of-coolant accidents (LOCAs) in light-water reactors and liquid-metal-coolant fast breeder reactors. The majority of the work reported has evidently been undertaken to obtain improved understanding of reactor LOCAs although much of the material is relevant to other situations in the power and process industries.

Participation in the meeting was by invitation: sixteen of the papers are from Japan, the remainder from the USA. The editors express the hope in the preface that the book will be a worthy sequel to the "Proceedings of the Symposium on Two-phase Flow Dynamics" held at Eindhoven in 1967. International participation has been severely restricted in this case; nevertheless the breadth and depth of the work reported is impressive. A significant number of leading US research workers in the field participated: Bergles, Weisman, Jones, Lahey, Bankoff and Henry contribute papers on those topics for which they are internationally recognised. There are some useful review articles among the US presentations.

Most of the work reported by the US participants is readily available and known to engineers and research workers in this field. Perhaps the major value of this book lies in the Japanese papers which report work less well known, even to those who read Heat Transfer–Japanese Research and other Japanese sources.

Recent work on two-phase flow, not restricted to dynamic aspects, in Japanese universities and colleges is summarised in an introductory paper. One hundred and eighty projects are reported, excluding activities on boiling heat transfer, packed beds, bubble columns, and gas–liquid chemical reactions. Thirty-seven universities and colleges have projects in this area. About the only topic I do not see here is that of two-phase flow across tube banks. Even the work on condensation appears confined to flow through tubes. Work on crossflow and many other topics is carried out by Japanese research organisations, other than universities. This book would have been enhanced if there had been a similar article on work in Japanese national institutions, institutes of research and private companies; an authoritative overview of Japanese work in this area has still to be written. The article by Nakanishi on Recent Japanese Research on Two-phase Flow Instabilities does in fact cover the three main research sectors, universities, research institutes and private companies.

The Japanese papers cover, among other topics, vertical bubble flow, the entrainment mechanism, dynamic characteristic of stratified flow, pressure wave propagation in plug flow, shock phenomenon in bubble and slug flow, vapour explosions, flow statility, and PWR reflood.

There is much of merit in this book for anyone concerned with two-phase flow and heat transfer.

D Chisholm
Glasgow College of Technology

Published, price $75.00, by Hemisphere Publishing Corporation, 1025 Vermont Avenue NW, Washington DC 20005, USA